Article ID: 1006-8775(2009) 01-0192-12

ANALYSES OF WIND STRUCTURE OF TYPHOON FUNG-WONG (2008) AND ITS RELATION TO PRECIPITATION REGION

ZHOU Yu-shu (周玉淑)[1], LIU Li-ping (刘黎平)[2]

(1. Laboratory of Cloud-Precipitation Physics and Severe Storms (LACS), Institute of Atmospheric Physics, Chinese Academy of Sciences, Beijing 100029, China; 2. State Key Laboratory of Severe Weather, Chinese Academy of Meteorological Sciences, Beijing 100081, China)

Abstract: Using real analysis data of 1°×1° resolution of the National Center for Environmental Prediction/National Center for Atmospheric Research (NCEP/NCAR), the nondivergent wind component and irrotational wind component obtained by the harmonic-cosine(H-C) method, and the wind structure of Typhoon Fung-Wong (coded 0808 in China) in 2008 was analyzed. The results indicated that the irrotational component was advantageous over the total wind in reflecting both the changes in convergent height and the asymmetrical convergence of Fung-Wong. In Fung-Wong, the nondivergent component was larger than the irrotational component, but the latter was much more variable than the former, which was obtained only from the wind partition method. Further analyses on the irrotational component demonstrated that the location of the convergent center at lower levels was almost the same as the divergent center during the development of Fung-Wong, and its convergent level was high in its life cycle, with the most highest up to 400 hPa when it became stronger. After the typhoon landed in the provinces of Taiwan and Fujian, respectively, its convergent center at lower levels was slowly detached from the divergent center at high levels and the convergent height was also depressed from high levels to lower levels. Gradually, this weakened the intensity of Fung-Wong. This kind of weakening was slow and Fung-Wong maintained its circulation for a long time over land because of its very thick convergent height. Analyses on wind partitioning provided one possible explanation to why Fung-Wong stayed for a long time after it landed. Furthermore, the asymmetric vertical ascending motion was induced by the asymmetric convergence at lower levels. In general, when typhoons (such as Fung-Wong) land, the rainfall region coincides with that of the convergence region (indicated by the irrotational component at lower layers). This means that the possible rainfall regions may be diagnosed from the convergent area of the irrotational component. For an observational experiment on typhoons, the convergent region may be considered as a key observational region.

Key words: wind partitioning; typhoon Fung-Wong; structure analysis

CLC number: P458.1.24 **Document code:** A **doi:** 10.3969/j.issn.1006-8775.2009.02.008

1 INTRODUCTION

China is a country with the most landed typhoons in the world. The typhoon is the main weather system that causes meteorological and secondary disasters[1]. The landed typhoon brings about storms and torrential rain, which causes great loss of life and property. Because of this, typhoon research is always an important topic in China. In the past few decades, a lot of investigations about typhoons (such as the movement mechanism, the prediction of path, the devolvement and intensity change, and the declination and maintenance after landing) have been carried out. Recently, the track prediction of typhoons has improved greatly while the intensity prediction does not improve as much as it should[2,3]. With the availability of satellites, new-generation Doppler weather radars, meteorological observation stations, improved observational methods, and accurate and multi-aspect services, much progress has been made in numerical

Received date: 2009-03-18; **revised date:** 2009-09-09

Foundation item: State Key Development Program for Basic Research of China (2009CB421505); Project of the Ministry of Sciences and Technology of the People's Republic of China (GYHY200706020); Projects of the Natural Science Foundation of China (40975034, 40775031); Open Project of State Key Laboratory of Severe Weather (2008LASW-A01)

Biography: ZHOU Yu-shu, PhD, undertaking mesoscale dynamical diagnosis and numerical modeling analyses. E-mail for correspondence author: zys@mail.iap.ac.cn

prediction, model development, and prediction of typhoon tracks. Since the 1990s, the errors in comprehensive prediction have gradually declined. In the prediction of structure and intensity, however, there is little improvement in China. With the development and widening use of mesoscale numerical prediction, the numerical simulation of typhoons has been increasing. Because the analysis of typhoon intensity and structure depends mainly on model output, it requires high precision and effectiveness in simulation. Recently, high time resolution data was widely used in the analysis of typhoons and mesoscale torrential rain systems[4,5], and some new variables were also used to study strong convection[6-12]. While many observational data, model output data, and variables, were now sufficient, what was lacking was a method to extract wind structure from the data. Setting up some kind of effective analysis method is important to understanding the typhoon's dynamical structure, intensity and its relation to the heavy rainfall region.

Aiming at the analysis of the structure of wind in Fung-Wong, the NCEP/NCAR real analysis data at 1° ×1° resolution was utilized, and the components of nondivergent wind and irrotational wind are obtained by the H-C method in the analysis of its wind structure.

2 H-C SERIES EXPANSION METHOD IN A LIMITED AREA

An effective technique to decompose the horizontal wind in a limited region is through calculating the streamfunction and velocity potential. The horizontal wind vector can be divided into the nondivergent and irrorational components based on the Helmholtz theory of

$$\vec{V} = \vec{V}_\psi + \vec{V}_\chi . \tag{1}$$

In Eq. (1), $\vec{V}_\psi = \vec{k} \times \nabla \psi$ is the nondivergent component, $\vec{V}_\chi = \nabla \chi$ the irrorational component, ψ the streamfunction, and χ the velocity potential. From Eq. (1), the streamfunction and velocity potential satisfy the following equations

$$\nabla^2 \psi = \Omega , \tag{2}$$

$$\nabla^2 \chi = D . \tag{3}$$

In Eqs. (2) & (3), Ω is the vorticity and D the divergence.

For the global atmosphere, Eqs. (2) & (3) can obtain a unique solution with periodic boundary. For a limited region, however, a stream field—which is both irrotational and nondivergent, i.e., its vorticity and divergence are equal to zero—cannot change the true streamfunction and velocity potential, making the solution of the Eqs. (2) & (3) less unique. In order to obtain a unique solution of the streamfunction and velocity potential in a limited area, restricted conditions other than those presented above should be included as well. Otherwise, problems such as calculation instability, the inability to reconstruct original wind, and the disappearance of systems at the boundary, may occur. Many scientists have tried to solve this issue of seeking solutions to Eqs. (2) & (3) with the boundary condition of Eqs. (4) and (5). In order to make the solutions consistent with a certain and proper distribution(i.e., the velocity potential remaining in accordance with the divergence and the streamfunction agreeing with the vorticity distribution), previous studies obtained the simple Dirichlet boundary condition, Neumann boundary condition, or various other kinds of condition combining these two types of boundary. In addition to the fact that the calculated precision could not be guaranteed, these techniques—also used in the mathematical sense—do not have accurate physical meaning. More recently, Lynch[13] pointed out that the solution of the streamfunction and velocity potential in a limited region was not unique and Chen and Kuo[14] gave an integrated mathematic justification about the unique question.

$$\vec{s} \cdot \vec{V} = \frac{\partial \psi}{\partial n} + \frac{\partial \chi}{\partial s} = v_s , \tag{4}$$

$$\vec{n} \cdot \vec{V} = -\frac{\partial \psi}{\partial s} + \frac{\partial \chi}{\partial n} = v_n . \tag{5}$$

Aiming at the unique issue in a limited area, Chen and Kuo[14,15] put forward two new methods, namely, the harmonic-sine series expansion method (H-S method) and the H-C method. In view of the fact that the streamfunction and velocity potential have no unique solutions in a limited area based on the mathematical equations, they redefined the criterion to estimate whether the solution was accurate or not. They pointed out that if the calculated streamfunction and velocity potential could reconstruct the original horizontal wind accurately, the solution of the streamfunction and velocity potential might be viewed as the final and unique result, which was a unique solution in the physical sense. The H-C method is physically significant in separating the horizontal wind in a limited region into internal and external components. The former only depends on the vorticity and divergence of the inner area while the latter is only associated with the outer area. In other words, the internal part is governed by a Laplace equation with non-zero boundary condition while the external one can be solved from a Poisson equation with homogeneous boundary values. When we seek mathematical solutions of these two kinds of differential issues, a harmonic function is appropriate for the external part

(therefore, it is also called harmonic part), and some kind of double-cosine series for the internal one. Using such an approach, it has been proved that the wind field reconstructed from the computed streamfunction and velocity potential in the limited region is able to fit well into the initial one, especially near the boundary. Additionally, calculation is proved to be quite efficient in the iterative procedure which is made up of no more than five iterative steps in total. Because there is no data in the Dirichlet boundary condition with which the streamfunction and velocity potential in meteorological observation can be calculated, the Neumann boundary condition adopted by the H-C method is more accurate in addressing meteorological questions. Supposing the limited area is a rectangle region *R*, and the boundary is a closed line *Σ*, the steps of the H-C method are listed briefly here for the integrality of our study. The detailed steps of the H-C method are shown as follows.

Step 1: Calculate the two-dimensional divergence D and vertical vorticity Ω using the observed wind in the limited rectangular area R with a closed boundary Σ.

Step 2: Solve the Poisson equations (6) under homogeneous boundaries (7),

$$\begin{aligned} \nabla^2\psi_{ic} &= \Omega \\ \nabla^2\chi_{ic} &= D \end{aligned}, \tag{6}$$

$$\begin{aligned} -\frac{\partial\psi_{ic}}{\partial y}+\frac{\partial\chi_{ic}}{\partial x} &= 0 \\ \frac{\partial\psi_{ic}}{\partial x}+\frac{\partial\chi_{ic}}{\partial y} &= 0 \end{aligned}, \tag{7}$$

where the inner part of streamfunction ψ_{ic} and velocity potential χ_{ic}, available by means of the inverse Fourier cosine transform operators from wave to physical space, can be obtained. Therefore, they are expressed in terms of double-cosine series. Here, the first subscript *i*(*I*) indicates the inner part while the second *c* denotes the cosine expansion. From Eq. (6), the inner part of the streamfunction ψ_{ic} and velocity potential χ_{ic} can be obtained by expanding the double Fourier-cosine function

$$\begin{aligned} \psi_{ic}(x,y) &= F^{-1}\left[\Phi_i(m,n)\right] \\ &= \sum_{m=1}^{M}\sum_{n=1}^{N}\Phi_i(m,n)\cos\frac{m\pi x}{L_x}\cos\frac{m\pi y}{L_y}, \end{aligned} \tag{8}$$

$$\begin{aligned} \chi_{ic}(x,y) &= F^{-1}\left[\mathrm{X}_i(m,n)\right] \\ &= \sum_{m=1}^{M}\sum_{n=1}^{N}\mathrm{X}_i(m,n)\cos\frac{m\pi x}{L_x}\cos\frac{m\pi y}{L_y}, \end{aligned} \tag{9}$$

where F^{-1} is the inverse Fourier transform operator, Φ and X are the double-cosine expanding series obtained by means of Fourier cosine transform in a limited area.

Step 3: Compute the horizontal wind components of the inner part, U_{Ic} and V_{Ic}, based on ψ_{ic} and χ_{ic} under the Helmholtz's theorem.

$$\begin{aligned} U_{Ic} &= -\frac{\partial\psi_{ic}}{\partial y}+\frac{\partial\chi_{ic}}{\partial x} = u_{I\psi}+u_{I\chi} \\ V_{Ic} &= \frac{\partial\psi_{ic}}{\partial x}+\frac{\partial\chi_{ic}}{\partial y} = v_{I\psi}+v_{I\chi} \end{aligned}. \tag{10}$$

Step 4: Derive the information about the external wind components, U_{Ec} and V_{Ec}, as in

$$U_{Ec} = U - U_{Ic},\quad V_{Ec} = V - V_{Ic}, \tag{11}$$

where the first subscript *E* stands for the external part.

Step 5: Calculate the coupled boundary conditions that are specified with the calculated U_{Ec} and V_{Ec}

$$\begin{aligned} -\frac{\partial\psi_{hc}}{\partial y}+\frac{\partial\chi_{hc}}{\partial x} &= U_{Ec} \\ \frac{\partial\psi_{hc}}{\partial x}+\frac{\partial\chi_{hc}}{\partial y} &= V_{Ec} \end{aligned}. \tag{12}$$

Then the two Laplace equations

$$\begin{aligned} \nabla^2\psi_{hc} &= 0 \\ \nabla^2\chi_{hc} &= 0 \end{aligned} \tag{13}$$

can be solved with an iterative method. Here the subscript *h* stands for the harmonic part. By the iterative method (for detailed calculation processes, see Chen and Kuo[14]), the harmonic parts of the streamfunction ψ_{hc} and velocity potential χ_{hc} are obtained.

Step 6: Utilize the calculated inner parts and harmonic parts from Eqs. (8) and (9) to obtain solutions to the streamfunction and velocity potential in a limited region

$$\psi = \psi_{ic} + \psi_{hc},\quad \chi = \chi_{ic} + \chi_{hc}. \tag{14}$$

Then, the nondivergent and irrotational wind components can be calculated by the streamfunction and velocity potential.

From the preceding six steps, one can see that the calculated solutions of the streamfunction and velocity potential have definite physical meaning: the inner part, ψ_i and χ_i, is determined by vorticity and divergence in the limited area with a homogenous boundary condition, which has no effect on the external part. The harmonic part, ψ_{hc} and χ_{hc}, is obtained by calculating the Laplace equations, which are determined by the boundary condition only, with its

maximum occurring just at the boundary. Compared from the order, the inner part is larger than the harmonic part. For this kind of iterative process, three to five steps are enough and the convergent velocity and calculated precision are improved more than with old methods.

3 A SIMPLE REVIEW OF TYPHOON FUNG-WONG

The best observational track of Fung-Wong (Fig. 1a), changes in the central minimum pressure (solid line in Fig. 1b) and the maximum velocity (dashed line in Fig. 1b) for the life cycle of Fung-Wong are shown in Fig. 1, which reflects the intensity of Fung-Wong at different positions and times. It is determined from its track and intensity that at 1400 LST (local standard time) 25 July 2008, Fung-Wong was moving westward, after forming over the ocean east of the Philippines. Subsequently, it evolved into a severe tropical storm at 0800 LST 26 July and became a typhoon at 2000 LST 27 July. After landing over the Hualian area of Taiwan Island at 0630 LST 26 July, Fung-Wong moved to the southeast coast with high winds, rain, and storm surge in the morning of 28 July. At 2200 LST 28 July, it landed at the town of Donghan in Fuqing city of Fujian Province with a central pressure of 975 hPa and maximum wind speed of nearly 33 m s^{-1}, and then moved northwestward but decreased gradually. On the night of 29 July, after staying over Fujian province for 23 hours, it moved into northeastern Jiangxi province. In the afternoon of 30 July, it weakened into a tropical depression in Panyang town of Jiangxi province. At 0200 LST 31 July, it was removed from the list of storm codes. Since its landfall on Fujiang province, Fung-Wong had stayed inland for about 52 hours.

It is shown from Fig. 1b that the strongest stage of Fung-Wong was from 2000 LST 27 to 0800 LST 28 July, with the center pressure at 955 hPa and maximum wind velocity at 45m s^{-1}. After landfall, the intensity of center pressure (975 hPa) was maintained for about 1 hour before declining to 980 hPa at 0000 LST 29 July (it stayed at 985 hPa from 0200 LST to 0700 LST 29 July). The center pressure of 990 hPa had been maintained for 23 hours since 0800 LST 29 July. The trend of the wind was similar to that of the pressure. After it declined in the form of a stepladder, the velocity of 23 m s^{-1} stayed for one day before weakening.

Seen from the satellite imagery, the cloud distribution of Fung-Wong was significantly asymmetric throughout its life cycle. The clouds in the southwest were dense and thick, which indicates that the water transfer was rich. Specifically, before Fung-Wong strengthened to a strong typhoon, its eye was not so clear (Fig. 2a); a clear eye and eyewall formed before it arrived at the island of Taiwan when the storm enhanced to a strong typhoon (Fig. 2b). After

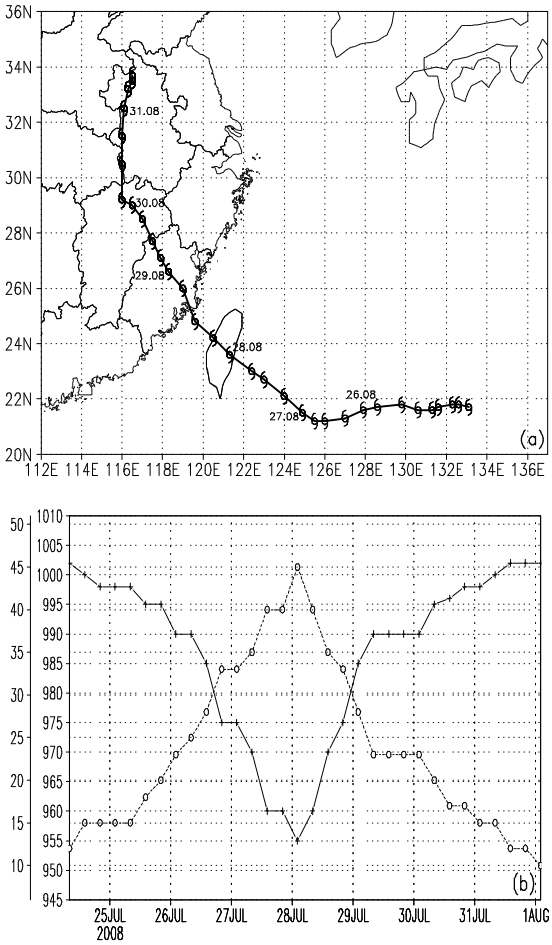

Fig.1 Best observational track (a), central minimum pressure (b, solid line, unit in hPa) and maximum velocity (b, dashed line, unit in m s-1) of Fung-Wong.

channeling its way across the island of Taiwan, Fung-Wong weakened to Category 1 but still posed a significant threat to coastal communities in mainland China. Having crossed the Taiwan Island with the center of the storm more or less traversing it through the middle part, the storm was headed toward the southeast coast. The crossing through the island disrupted its shape and strength. The eye was still evident but no longer clear and well-formed (Fig. 2c). After it landed at Fujian province again, its eyewall and spiral structure of clouds were destroyed (Fig. 2d) but the vortex structure persisted longer.

Being the first strong typhoon that landed in China in 2008, Fung-Wong is characterized by its large size, wide-range influence, and high water vapor content. Particularly, its shape was imbalanced with clouds primarily present to the south of the eye during the early stage. The thick clouds were always located at

the southeastern quadrant. Supported by plenty of water vapor supply, it produced torrential rain that was large in intensity, coverage, and impact. It represents a typical case study for us to investigate typhoons well-known for structure and intensity in China.

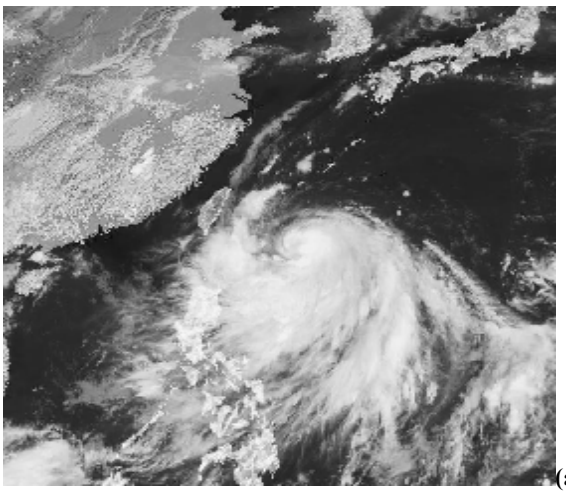

(a)

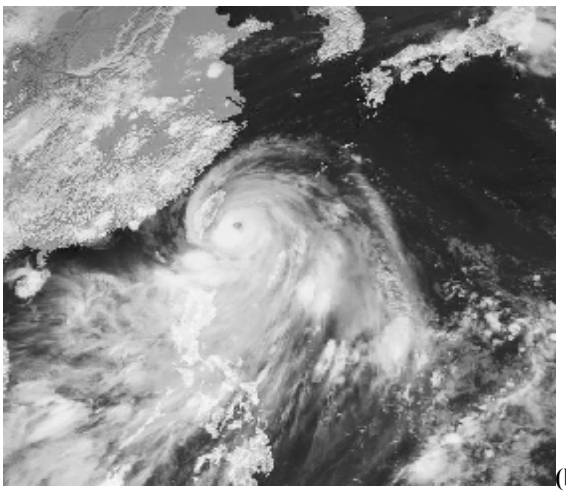

(b)

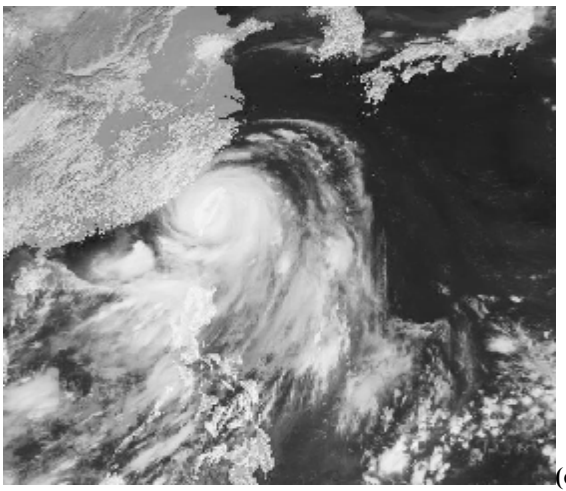

(c)

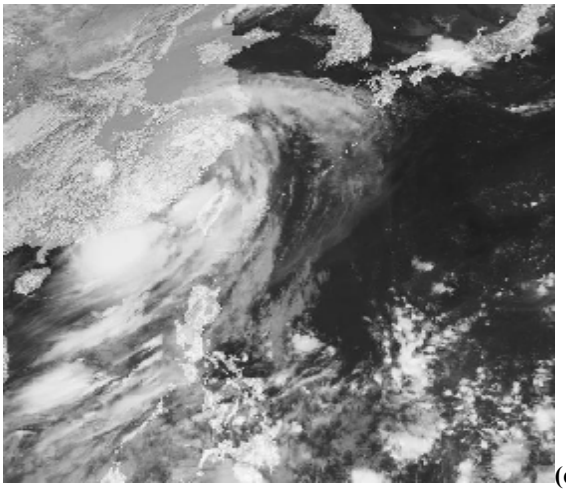

(d)

Fig.2 Cloud images at 1400 LST on 26 July (a), at 2000 LST on 27 July (b), at 0800 LST on 28 July (c), and at 0800 LST on 29 July (d), 2008.

4 SYNOPTIC PATTERN AND WIND-FIELD STRUCTURE OF TYPHOON FUNG-WONG

According to the basic steps of the H-C method listed above, and with the use of real analysis data of 1°×1° resolution of NCEP/NCAR, the wind structure of Fung-Wong is analyzed.

4.1 *Synoptic pattern of Typhoon Fung-Wong*

In the development stage of Fung-Wong, a strong South Asian High controlled the area of East Asia (figure omitted). In the early stage of Fung-Wong's formation, there was a typical pattern of two troughs and one ridge at the 500 hPa weather chart of East Asia (Fig. 3a). One of the troughs — in a southwest-northeast direction — was near eastern Europe and the other in eastern Mongolia with one high pressure extended from the Baikal Lake to eastern Russia. At the rear of the high, two cutoff lows appeared in northeastern Japan and Bohai Bay respectively. The 588 isoline (in unit of dgpm) remained over the western Pacific, whereas its main body had spread into middle and eastern China. Fung-Wong was generated near a low pressure of convex to the south of the west Pacific subtropical high, where a high-temperature zone corresponded to the center of the subtropical high. At 2000 LST 20 July (Fig. 3b), the circulation pattern did not change much in mid- and high-latitude and the two troughs deepened in eastern Europe and eastern Mongolia, accompanied with a closed center. A low at the Bohai Bay moved to the Korean Peninsula where the subtropical high deepened. Due to the persistence of the two lows in

mid- and high-latitude, the subtropical high hardly shifted northward but instead extended westward. Fung-Wong moved westward along the easterly current south of the subtropical high. At 0800 LST of 26 July (figure omitted), both the trough and ridge of the subtropical high moved to the west by about 2.5 longitudes; compared to 2000 LST of 25 July, low pressure controlled the areas of northeastern Inner Mongolia and Korean Peninsula, which faced right with the subtropical high. By 0800 LST 27 July (Fig. 3c), the main body of the subtropical high had strengthened continuously and the 588 isoline had extended to Jiangsu and Zhejiang provinces while the control range of the 586 isoline shrank. In the west Pacific, the subtropical high gradually moved southward and its ridge line turned from east-west to northwest-southeast. By 2000 LST of 27 July (figure omitted), the 588 isoline had moved northwestward to the north and northeast of China as its ridge line took on a northwest-southeast direction. Along the southern edge of the subtropical high, Fung-Wong moved to the island of Taiwan with the northeast airflow outside the subtropical high. At 0800 LST 28 July (Fig. 3d), a trough, previously in eastern Europe, shifted to the east of Mongolia while the main body of the subtropical high still maintained a northwest-southeast direction. After landfall on the island, Fung-Wong, owning to the steering flow of the subtropical high, continued its northwestward motion. From 0800 LST of 29 July, as the 588 isoline retreated eastward, Fung-Wong was located to the west of the subtropical high and its path recurved to the north accordingly.

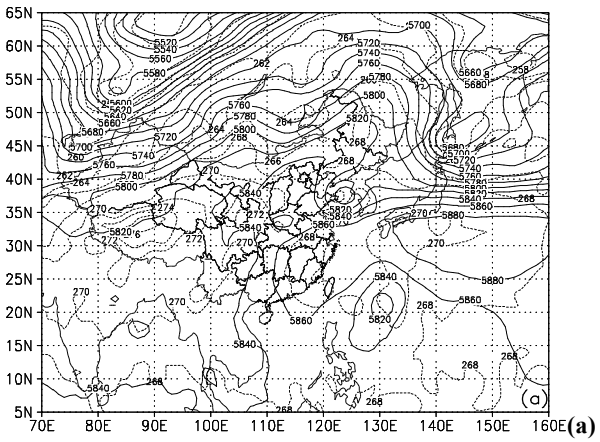

(a)

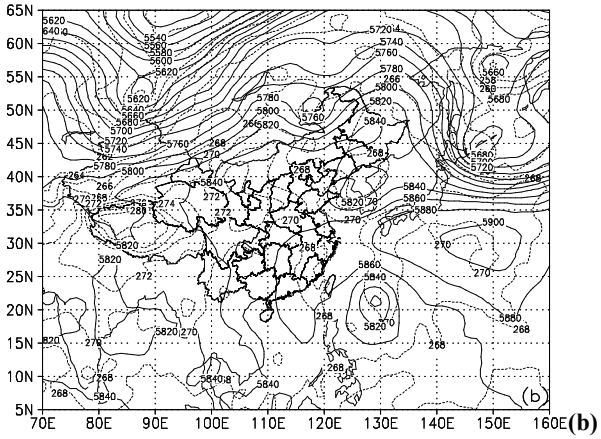

(b)

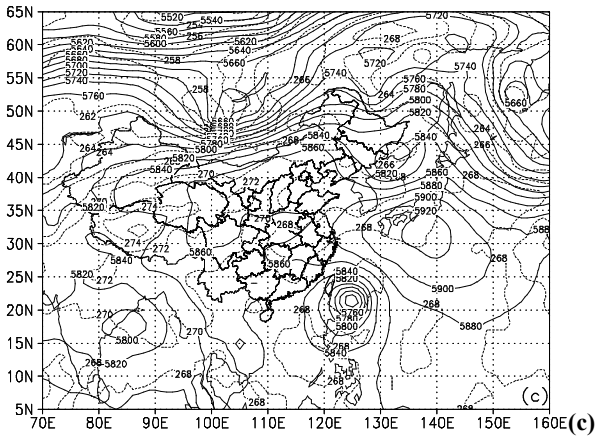

(c)

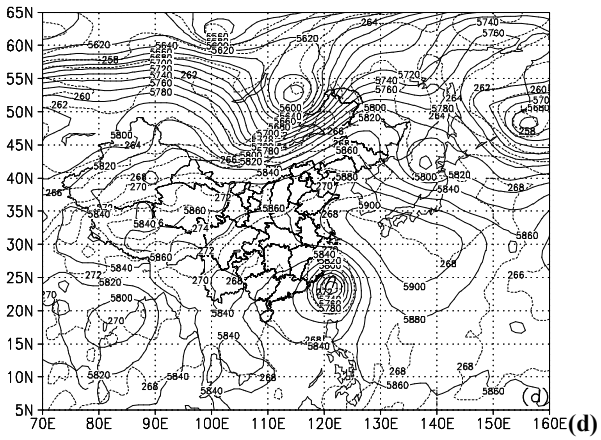

(d)

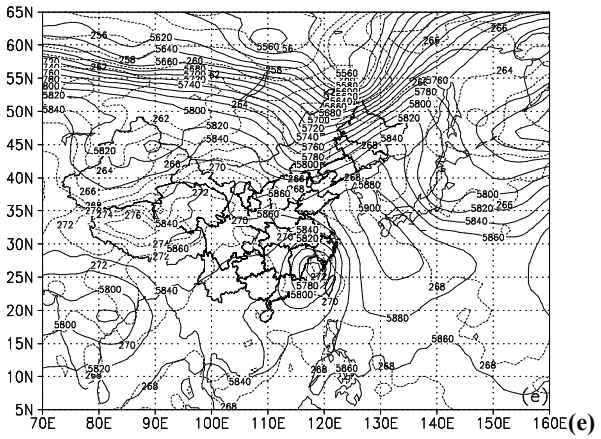

(e)

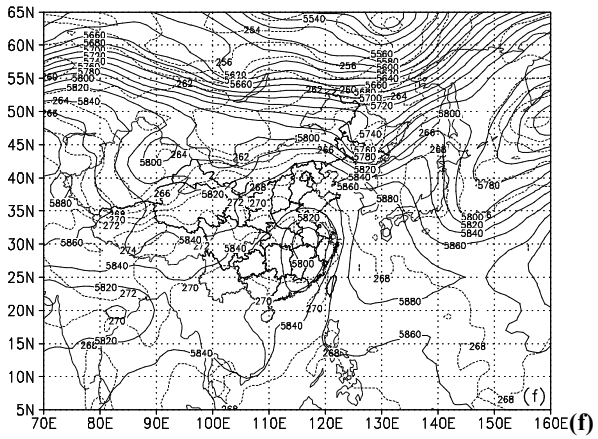

Fig.3 Distribution of geopotential height (solid line, unit in dgpm) and temperature (dashed line, unit in K) at 0800 LST 25 July, 2008 (a), 0800 LST 27 July (b), 0800 LST 28 July (c), 0800 LST 29 July (d), 0800 LST 29 July (e), and 0800 LST 30 July (f), at the level of 500 hPa.

It is known from the weather charts of 500 hPa that the moving path of Fung-Wong was mainly influenced by the flow outside of the west Pacific subtropical high. Located to the south of the subtropical high, Fung-Wong took a primarily westward path in the early stage. When it recurved to the southwest of the high, its path shifted to the northwest direction. After the typhoon moved to Jiangxi province, it was to the west of the subtropical high and the path changed to the north direction. In all, the path of Fung-Wong was greatly influenced by the subtropical high. Moreover, in the moving and developing processes, the water vapor from the southerly and easterly areas outside the subtropical high was entrained into Fung-Wong, supplying sufficient amount of moisture.

4.2 *Wind distribution of Typhoon Fung-Wong*

Based on the maintenance of circulation and a plentiful moisture supplement, the wind structure of Fung-Wong is further analyzed in this section. By using real analysis data of $1° \times 1°$ resolution of NCEP/NCAR and applying the harmonic-cosine method to partition horizontal wind associated with the path of Fung-Wong, we found that in the development of Fung-Wong, a convergent center coincided with a vortex center at mid- and lower-levels and a convergent center at lower levels also coincided with a divergent center at high levels. This acted as a dynamic pump that lifted the water vapor from lower levels to mid- and higher-levels. This was one of the reasons why Fung-Wong had long life span and caused torrential rain and floods. Besides, by comparing the irrotational component of different levels in contrast with the intensity of Fung-Wong at corresponding time, we can conclude that when the convergent center was lifted up to 500 hPa, Fung-Wong continuously developed and could reach the category of strong typhoons. When the convergent center decreased, the strength of Fung-Wong declined as well. Therefore, in the different stages of Fung-Wong's life cycle, the irrotational component varies significantly, which was a feature of its horizontal wind field from the perspective of wind partition.

In all stages of Fung-Wong's life cycle, the distribution of the nondivergent component was close to that of the total wind. To take an obvious example, when Fung-Wong grew to become a stronger typhoon at 0200 LST 28 July, the nondivergent component (Fig. 4b) was almost equivalent to the total wind (Fig. 4a) while the order of the irrotational component was far less than that of the nondivergent component. This indicated that with Fung-Wong, the quasi-geostrophic component still played a predominant role while its asymmetric structure depended on both the irrotational component and nondivergent component. The asymmetric structure of the nondivergent component emerged on the east and west sides of typhoon circulation, whereas that of the irrotational component emerged on the north and south sides. This was different from Typhoon Saomai, whose asymmetric structure was decided mainly by the nondivergent component[16]. Moreover, in the different stages of Fung-Wong, changes in the nondivergent component were less than those of the irrotational component, showing that the intensity of Fung-Wong depended mainly on the variation of the irrotational component. So, in the following part, the distribution of the irrotational component is emphasized in the various stages of Fung-Wong.

In the developing stage, there was convergent motion below 850 hPa, with obvious changes between 700 hPa and 500 hPa. In this aspect, therefore, the change in the irrotational component between 700 hPa and 500 hPa was emphasized. For high levels, 200 hPa is studied intensively as an example. At 0800 LST 25 July, Fung-Wong was a tropical depression and there was obvious convergence of the irrotational component (figure omitted) from 1000 hPa to 700 hPa. Moreover, the lower the level was, the more obvious the convergence was. At lower levels, the center of convergence was located around the Fung-Wong center. At 600 hPa, weak convergent zones were situated behind the typhoon while there was weak divergence above 400 hPa. By 0800 LST 26 July (figure omitted), Fung-Wong had grown up to become a strong tropical storm but obvious convergence still existed near its center at 700 hPa and 600 hPa. At 500 hPa, wind convergence emerged on the right side of the center and these convergence motions were located near the west and south of the typhoon. At 200 hPa, large areas of

divergence played a predominate role outside the South Asia high while there was weak divergent current above Fung-Wong, which indicated that a configuration had formed where there was convergence at lower levels and divergence at higher levels.

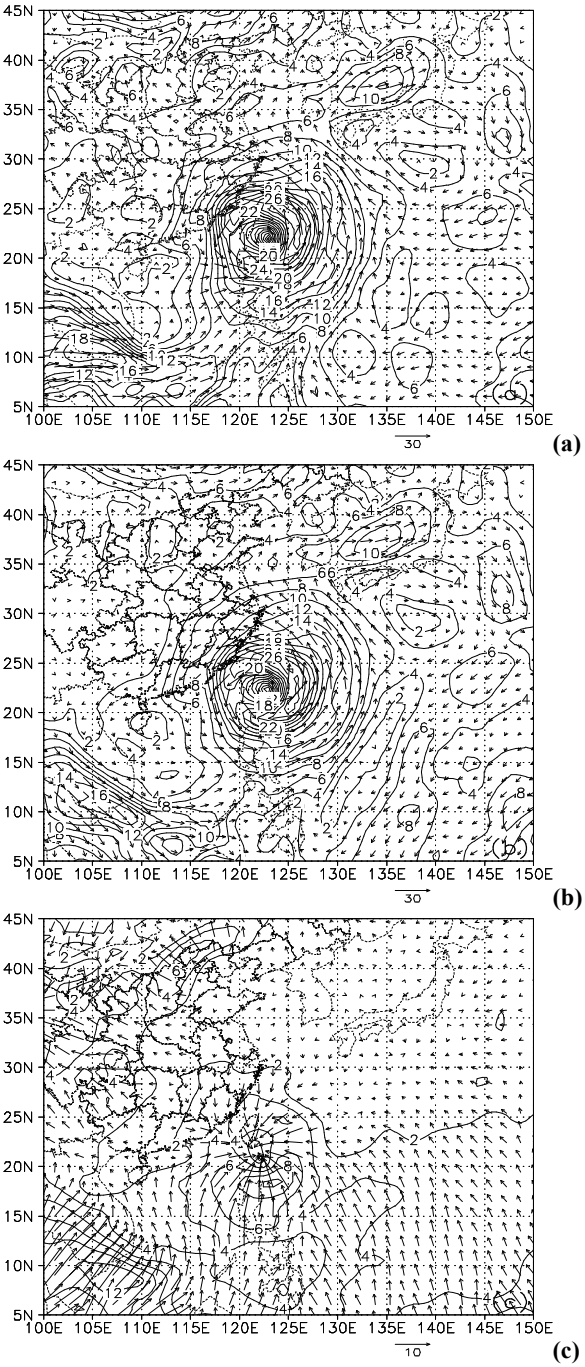

Fig.4 Distribution of total wind (a), nondivergent component (b), and irrotational component (c) on 850 hPa at 0200 LST 28 July, 2008.

By 0800 LST July 27, Fung-Wong had developed into the category of typhoon. Compared to the situation of 0800 LST 26 July, the convergence continued strengthening at 700 hPa and 600 hPa. Near the Fung-Wong center, the isoline of the irrotational component increased from 2 m s^{-1} to 4 m s^{-1}, but was different from the situation of 0800 LST 26 July when the convergence was located at the south and west of the typhoon. On 27 July, the convergence on the east and north sides also intensified as the airflow went into the eye from all around (Fig. 5a & b). Significant variations of convergence happened at the middle level of the troposphere, such as 500 hPa, and the convergent wind on the south of Fung-Wong increased from 2 m s^{-1} at 0800 LST 26 July to 6 m s^{-1} at 0800 LST 27 July. The convergence also took on a substantially asymmetric structure, i.e., the intensity on the southeast was greater than on the northwest (Fig. 5c). At 200 hPa, divergence also reinforced with the irrotational component increasing swiftly from 6 m s^{-1} to 16 m s^{-1} (Fig. 5d). Owing to the much higher convergent level of Fung-Wong, the deep convergence — with the highest level at 300 hPa – 400 hPa—was quite distinct from Typhoon Saomai in 2006. In Saomai, the convergent level was low with the significant level at 1000 hPa – 925 hPa. It was marked by a thin convergence layer at lower levels and a thick divergence layer at mid- and-higher levels, which led to very strong wind at lower levels. Furthermore, in Fung-Wong, the 200-hPa divergence in the southeast was larger than in the northwest, based on the lower level convergence. The reinforced mid- and low-level convergence and high level divergence were consistent with the intensification of Fung-Wong, which was demonstrated to associate Fung-Wong with the configuration of its dynamics. Corresponding to the reinforced irrotational component, the vertical motion near the eye wall of Fung-Wong increased as well (Fig. 6a). The maximum upward velocity zone, relative to the strong convergence and divergence to the south of typhoon, was also located in the south of Fung-Wong. The vertical motion was asymmetric: to the south of the typhoon at 18°N – 20°N, there was a strong upward motion (with a center of 2.0 Pa s^{-1}); to the north, near the eye wall, the maximum upward velocity was only 0.6 Pa s^{-1}. So, in the circulation of Fung-Wong, the asymmetric horizontal convergence and divergence dictated the asymmetric vertical motion. It is known from Fig. 6a that at this moment, the vertical motion of Fung-Wong was similar to other typhoons. Namely, there was downward motion in the inner eye and upward motion near the eye wall.

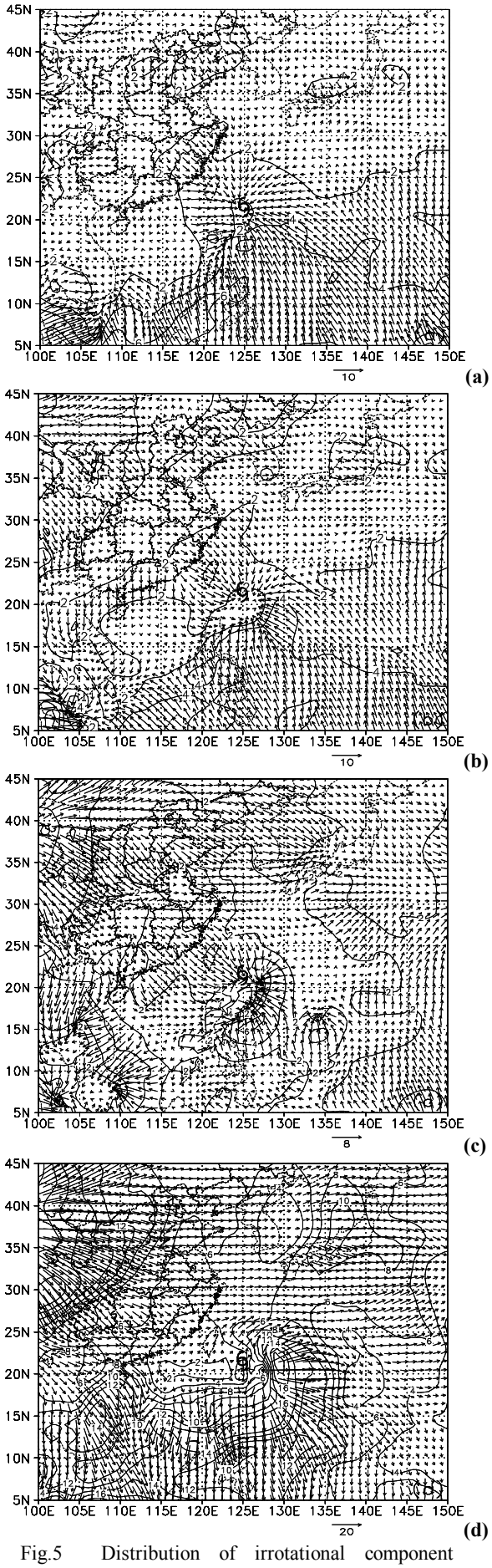

Fig.5 Distribution of irrotational component (vector, unit in m s^{-1}) and velocity (contour) at 0800 LST 27 July at 700 hPa (a), 600 hPa (b), 500 hPa (c), and 200 hPa (d). The typhoon symbol represents the typhoon center at the corresponding time.

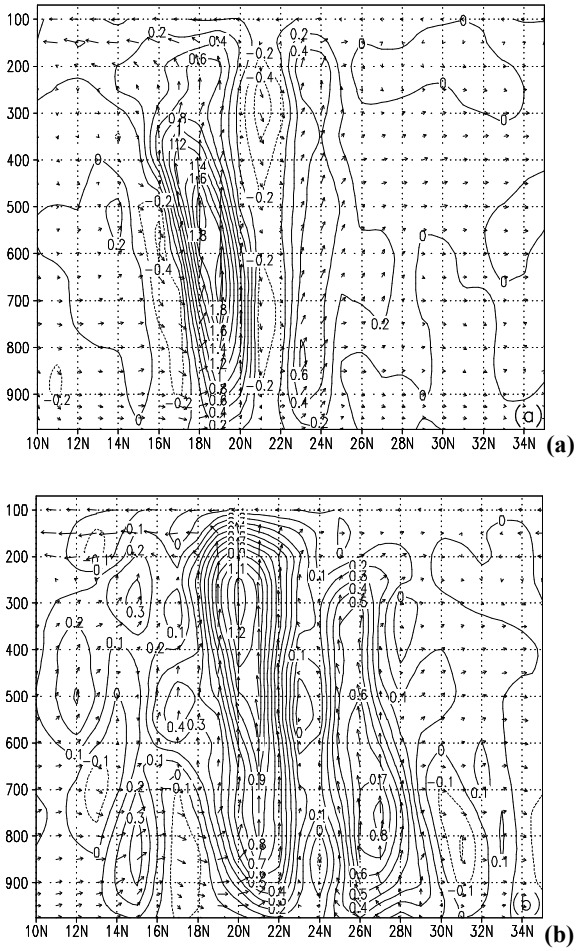

Fig.6 Longitude-pressure section along the typhoon center of vertical velocity (contour, unit in Pa s–1) and ũw×25 (vector) at 0800 LST 27 July (a) and 0800 LST July (b) 2008.

At 0800 LST 28 July (Fig. 7), Fung-Wong landed on the island of Taiwan as a strong typhoon (at 0630 LST 28 July) and the convergent situation was similar to that of 0800 LST 27 July. Convergence existed below 500 hPa while divergent wind decreased from 4 – 6 m s^{-1} to 2 – 4 m s^{-1} (Fig. 7c). At 200 hPa, there was still strong divergence above the center of Fung-Wong. It is seen from the vertical circulation that, although the strong upward motion maintained near the eye wall and the vertical motion in the south was larger than in the north, the downward motion decreased in the eye wall. Especially (as shown in Fig. 7b), the downward motion was not significant, which showed that the circulation of Fung-Wong was influenced by the Taiwan Island's topography and its dynamical structure also changed accordingly.

At 2200 LST 28 July, Fung-Wong landed again on

Fujian province as a typhoon, with the convergence in the mid- and lower-level being similar to that before landing (convergence existed below 500 hPa while divergent wind decreased 4－6 m s^{-1} to 2－4 m s^{-1} (figure omitted). At 200 hPa, there was still strong divergence. At 0000 LST 29 July, under 700 hPa, the circulation center of Fung-Wong sill existed but at 600 hPa－500 hPa, the uniform convergence center did not exist any longer. Instead, there was a convergent line to the east of Fung-Wong (figure omitted). The divergence center of 200 hPa was not located above the center of Fung-Wong any more; instead, it was moving to the southwest. In short, after the second landing, the convergent motion maintained beneath 700 hPa while the convergence declined in the middle level. From the lower level to the high level, the center of convergence and divergence did not agree with each other upright but inclined instead. Accordingly, Fung-Wong had declined into a tropical storm with a long life span. At 0800 LST 30 July (figure omitted), the convergence areas at 700 hPa and 600 hPa moved to the northeast of the center of the storm, the convergence center at 500 hPa moved to the coastal line of Zhejiang province and there was nondivergent flow above Fung-Wong. While at 200 hPa, the strong divergent center had moved to the south of China, its convergent center at lower levels detached further from the divergent center at high levels. Because the convergence remained at 600 hPa, the layer of convergence was very thick and Fung-Wong weakened gradually. At 0800 LST 31 July (figure omitted), below 850 hPa, convergence still existed but convergence at 700 hPa and 600 hPa continued to decrease and nondivergent current dominated above 500 hPa. So, with the lowering of the convergence layer, after landing and moving to the north, Fung-Wong declined in intensity as well. Due to the thick convergence layer, Fung-Wong weakened slowly and maintained for a long time after landfall.

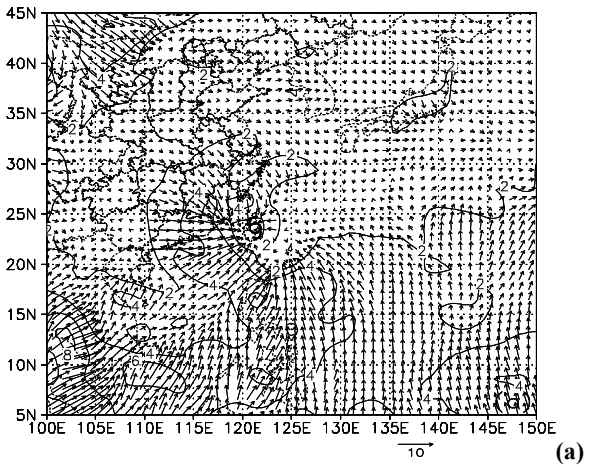

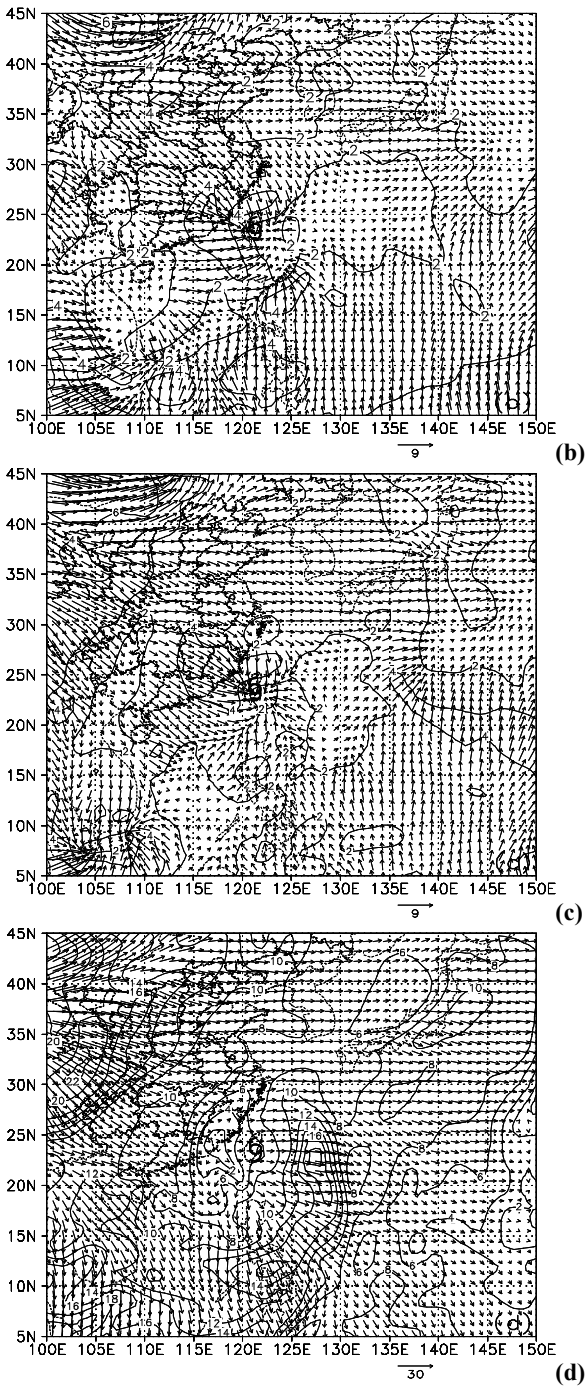

Fig.7 Same as Fig.5 except for 0800 LST 28 July, 2008.

Seen from the rainfall at 6h interval (shaded region in Fig. 8) with the distribution of the irrotational component (vector arrows in Fig. 8), both before (Fig. 8a, b) and after (Fig. 8c, d, e, f) Fung-Wong landed, the precipitation center generally coincided with the center of the irrotational component of Fung-Wong at lower levels (the irrotational component at 850 hPa was taken as an example in Fig. 8). Sometimes, like the situation in Fig. 8f, the rainfall center was not located right above the convergence center, but was still within the convergent region. Therefore, from the distribution of the irrotational component under 850 hPa, we can

estimate the possible rainfall region approximately. It is necessary to point out that when the vortex moved further inland, the factors impacting the rainfall were more than those at sea and the precipitation should not be located in the convergent center any more. For Typhoon Fung-Wong, if observation was done before its landing, the convergent region indicated by its irrotational component at lower levels may be taken as a factor to select the key observational region.

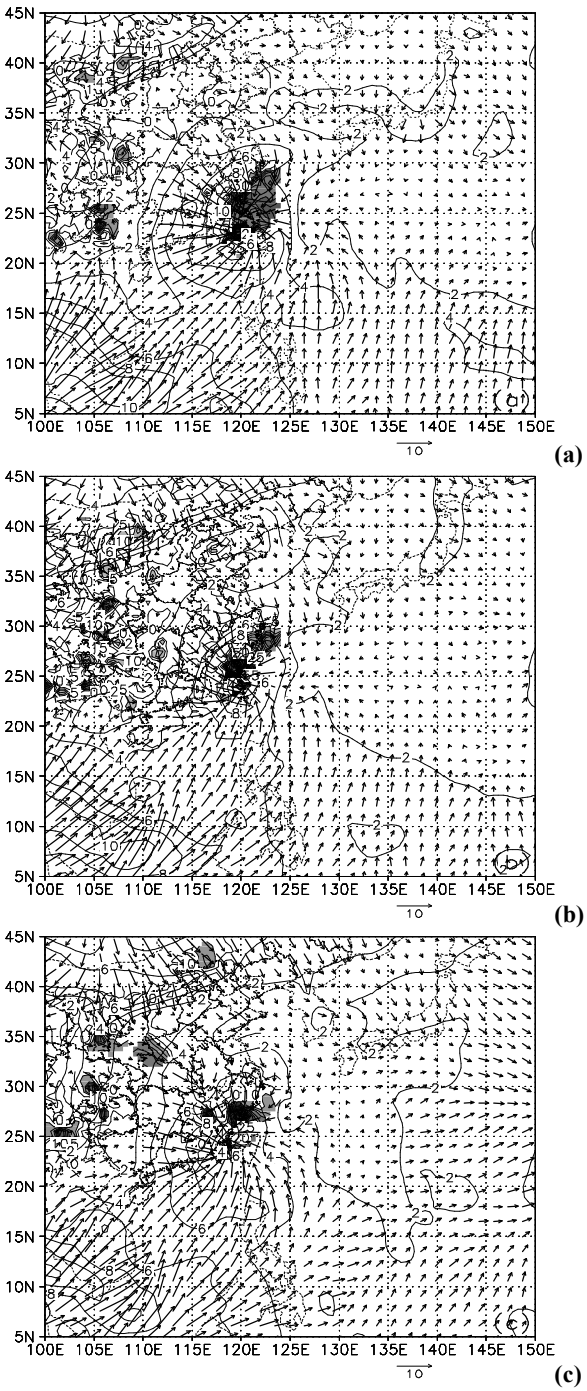

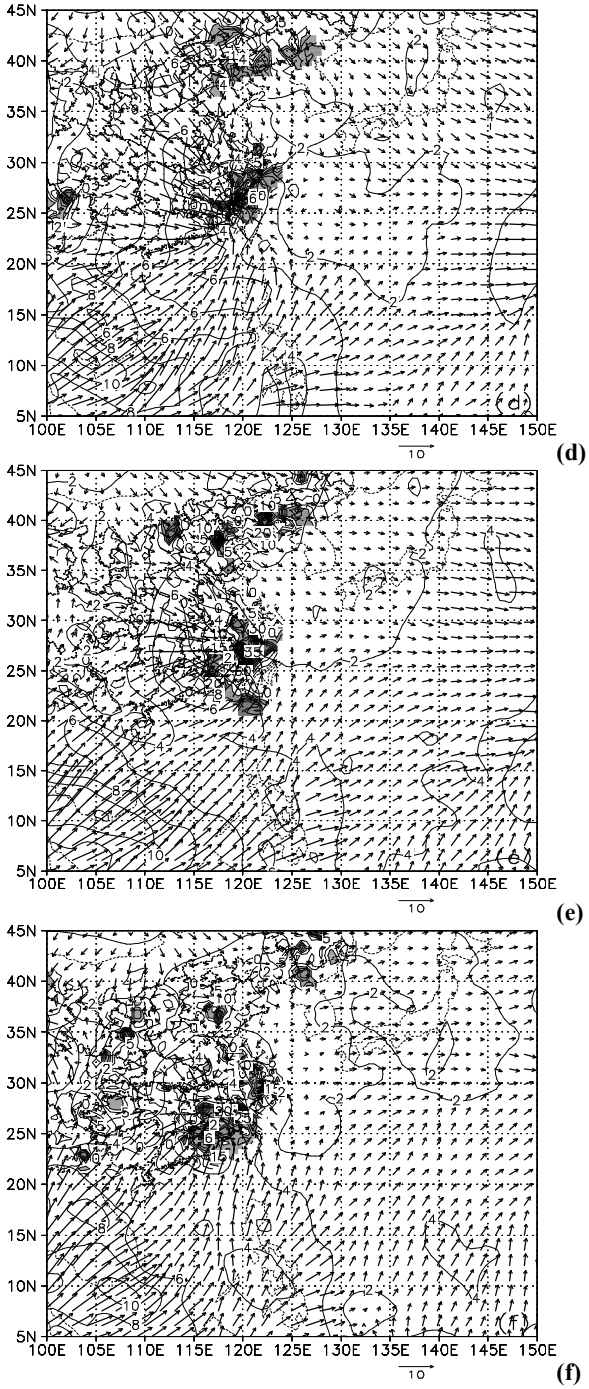

Fig.8 Rainfall amount with 6-h intervals (shaded, unit in mm) and the irrotational component (vector) at 1400 LST 28 July (a), 2000 LST 28 July (b), 0200 LST 29 July (c), 0800 LST 29 July (d), 1400 LST 29 July (e), and 2000 LST 29 July (f), 2008.

5 DISCUSSION AND CONCLUSION

Applying the harmonic-cosine method, the nondivergent wind component and irrotational wind component were obtained. Using the real time routine weather chart and real analysis data with $1° \times 1°$ resolution of NCEP/NCAR, the wind structure of typhoon Fung-Wong (No. 200808) was analyzed. We

got more information on the nondivergent wind component and the irrotational wind component than we did with the original wind, which reflects the dynamic features of lower level convergence and higher level divergence, asymmetrical structure of horizontal convergence, corresponding asymmetrical vertical motion, and the variation of convergence layer (which was a supplement of total wind). The result indicated that in typhoon Fung-Wong, the nondivergent component was larger than the irrotational component, but the variety of the irrotational component was more significant than that of the nondivergent component. Further analyses showed that as it landed in Taiwan and Fujian Provinces, its convergent center at lower levels was slowly detached from the divergent center at higher levels. Due to the thick layer of convergence and the convergent motion declining from the higher layer to the lower layer, Fung-Wong was weakened gradually and remained for a long time. This is a possible explanation, from the perspective of wind partitioning, why Fung-Wong could remain a long time after landing. In general, the rainfall region coincided with the convergence region indicated by the irrotational component below 850 hPa. This means that one can deduce the possible rainfall regions from the convergence area, especially for the neighboring area of convergent center at lower levels. For typhoon observational experiments (combined with other methods), the convergent region at lower levels may be taken as a factor to determine the key observational region.

In this paper, although we have employed a simple synoptic partition, the method of wind field partition is a good supplement and improvement to the weather analysis and diagnosis. Now, with only the horizontal wind partitioned, understanding how to combine this with the vertical wind component to explain the dynamical mechanism, and understanding how to deal with the three-dimensional stream field analysis are the key areas of work in future.

REFERENCES:

[1] CHEN Lian-shou, DING Yi-hui. Introduction on West Pacific Typhoon [M]. Beijing: Science Press, 1979: 462-474.
[2] CHENG Zheng-quan, CHEN Lian-shou, XU Xiang-de. Research progress on typhoon heavy rainfall in China for last ten years [J]. Meteor. Mon., 2005, 31(12): 3-9.
[3] CHEN Lian-shou. The evolution on research and operational forecasting techniques of tropical cyclones [J]. J. Appl. Meteor. Sci., 2006, 17(6): 672-681.
[4] DENG Guo, ZHOU Yu-shu, LI Jian-tong. The experiments of the boundary layer schemes on simulated typhoon part I. the effect on the structure of typhoon [J]. Chin. J. Atmos. Sci., 2005, 29: 417-428.
[5] LI Bai, ZHOU Yu-shu, ZHANG Pei-yuan. Application of the China New Generation Weather Radar data to the torrential rain simulation over the Jianghuai Basin in 2003: Validation of precipitation and wind [J]. Chin. J. Atmos. Sci., 2007, 31(5): 826-838.
[6] GAO Shou-ting, LEI Ting, ZHOU Yu-shu. Diagnostic analysis of moist potential vorticity in torrential rain systems [J]. J. Appl. Meteor. Sci., 2002, 13: 662-670.
[7] GAO Shou-ting, LEI Ting, ZHOU Yu-shu. Moist potential vorticity anomaly with heat and mass forcings in torrential rain systems [J]. Chin. Phys. Lett., 2002, 19: 878-880.
[8] GAO S, WANG X, Zhou Y. Generation of generalized moist potential vorticity in a frictionless and moist adiabatic flow [J]. Geophy. Res. Lett., 2004, 31, L12113, doi: 10.1029/2003GL019152.
[9] GAO Shou-ting, ZHOU Yu-shu, CUI Xiao-peng. Impacts of cloud-induced mass forcing on the development of moist potential vorticity anomaly during torrential rains [J]. Adv. Atmos. Sci., 2004, 21(6): 923-927.
[10] GAO Shou-ting, ZHOU Yu-shu, LEI Ting. Analyses of hot and humid weather in Beijing city in summer and its dynamical identification [J]. Sci. in China (Ser. D), 2005, 48: 128-137.
[11] GAO S, CUI X, ZHOU Y, LI X. A modeling study of moist and dynamic vorticity vectors associated with two-dimensional tropical convection [J]. J. Geophys. Res., 2005, 110, D17104, doi: 10.1029/2004JD005675.
[12] GAO S, Ran L. Diagnosis of wave activity in a heavy-rainfall event [J]. J. Geophys. Res., 2009, 114, D08119, doi: 10.1029/2008JD010172.
[13] LYNCH P. Partitioning the wind in a limited domain [J]. Mon. Wea. Rev., 1989, 117: 1492-1500.
[14] CHEN Q S, KUO Y H. A harmonic-sine series expansion and its applation to the partitioning and reconstruction problem in a limited area [J]. Mon. Wea. Rev., 1992, 120: 91-112.
[15] CHEN Q S, KUO Y H. A consistency condition for the wind field reconstruction in a limited area and a harmonic-cosine series expansion [J]. Mon. Wea. Rev., 1992, 120: 2653-2670.
[16] ZHOU Yu-shu, CAO Jie, GAO Shou-ting. The method of decomposing wind field in a limited area and its application to typhoon SAOMEI [J]. Acta Phys. Sin-Ch Ed, 2008, 57(10): 6654-6665.

Citation: ZHOU Yu-shu and LIU Li-ping. Analyses of wind structure of typhoon Fung-Wong (2008) and its relation to precipitation region. *J. Trop. Meteor.*, 2009, 15(2): 192-203.